International Journal of Marine Energy 19 (2017) 16–31

Contents lists available at ScienceDirect

International Journal of Marine Energy

journal homepage: www.elsevier.com/locate/ijome

Parametric FEA modelling of offshore wind turbine support structures: Towards scaling-up and CAPEX reduction

Maria Martinez-Luengo, Athanasios Kolios *, Lin Wang

Cranfield Energy, Cranfield University, Bedford MK43 0AL, UK

ARTICLE INFO

Article history:
Received 30 November 2016
Revised 29 April 2017
Accepted 24 May 2017
Available online 26 May 2017

Keywords:
Offshore wind turbines
Structural health monitoring
Key design parameters
Structural integrity

ABSTRACT

Parametric Finite Element Analysis (FEA) modelling is a powerful design tool often used for offshore wind. It is so effective because key design parameters (KDPs) can be modified directly within the python code, to assess their effect on the structure's integrity, saving time and resources. A parametric FEA model of offshore wind turbine (OWT) support structures (consisting of monopile (MP), soil-structure interaction, transition piece (TP), grouted connection (GC) and tower) has been developed and validated. Furthermore, the different KDPs that impact on the design and scaling-up of OWT support structures were identified. The aim of the analyses is determining how different geometry variations will affect the structural integrity of the unit and if these could contribute to the turbine's scale-up by either modifying the structure's modal properties, improving its structural integrity, or reducing capital expenditure (CAPEX). To do so, three design cases, assessing different KDPs, have been developed and presented. Case A investigated how the TP's and GC's length influences the structural integrity. Case B evaluated the effect of size and number of stoppers in the TP, keeping a constant volume of steel; and Case C assessed the structure's response to scour development. It is expected that this paper will provide useful information in the conceptual design and scale-up of OWT support structures, helping in the understanding of how KDPs can affect not only the structure's health, but also its CAPEX.

1. Introduction

In 2007 the European Union set particular and challenging goals to all Member States, establishing that by 2020 the UK must produce 15% of its energy consumption from renewable energy sources. Wind energy is probably the most promising technology contributing to decarbonisation within the UK; in fact, its growth over the last decade confirms this. According to Renewable UK [1], 1.4 GW were installed offshore in 2015 in the UK, making the total Wind Energy capacity 13.3 GW. In other words, wind energy alone provides more renewable electricity than all other sources combined.

According to [2] offshore wind (OW) deployment could reach 20–55 GW by 2050. Nowadays and for the next few years mature fixed-bottom technology will dominate, exploiting shallow and close-shore sites, which can be installed at low cost. Beyond 20 GW, fixed-bottom turbines will be forced to move further from shore to access suitably shallow waters, creating numerous challenges. Floating wind (FW) would mitigate some of these challenges, making deep water sites close to shore suitable. In fact, a contribution between 8 and 16 GW of floating is expected if the 40GW of offshore wind deployment is

* Corresponding author.
E-mail address: a.kolios@cranfield.ac.uk (A. Kolios).

http://dx.doi.org/10.1016/j.ijome.2017.05.005
2214-1669/

Nomenclature

Acronyms

ALS	Accidental Limit State
API	American Petroleum Institute
CAPEX	Capital Expenditure
EOC	Environmental and Operational Conditions
FEA	Finite Element Analysis
FLS	Fatigue Limit State
FW	Floating Wind
GC	Grouted Connection
KDP	Key Design Parameter
KPI	Key Performance Indicator
LCOE	Levelised Cost of Energy
MP	Monopile
MSA	Maximum Stresses Allowed
MUR	Maximum Utilisation Rate
OMA	Operational Modal Analysis
OW	Offshore Wind
OWT	Offshore Wind Turbine
O&M	Operations and Maintenance
SLS	Serviceability Limit State
SHMS	Structural Health Monitoring Systems
TP	Transition Piece
ULS	Ultimate Limit State

reached. Despite all the advantages, FW technology has yet to be demonstrated at large scale and to face the challenge of driving costs down. A number of cost projections suggest that FW can reach cost parity with fixed-bottom during the 2020s if adequate support is provided by government. Another study [3] suggests that leading FW concepts could achieve a Levelised Cost of Energy (LCOE) of £85-95/MWh in large-scale commercial projects, with further cost reduction possible over time.

This trend in increasing wind farm capacity will not only be maintained in the following years, but also a progressive increase in offshore wind turbine (OWT) size is expected [4]. OWT capacity has grown by 41.1% from 2010 to 2015. In 2015, the average capacity of new OWTs installed was 4.2 MW, a significant increase from 3.0 MW in 2010, reflecting a period of continuous development in turbine technology to increase energy yields offshore. The deployment of 4–6 MW turbines seen in 2015 will be followed by the gradual introduction of 6–8 MW turbines closer towards 2018 [5].

With this rapid growth in capacity and size, the scale-up of OWTs presents some issues that need to be assessed. A couple of these are the interference between the structure's modal frequencies, with the rotor and environmental excitations and the trade-off between the increase in power and its economic cost. Designing OWTs is challenging due to the dynamic sensitivity of the structures. The reason is the proximity of these structures' natural frequencies to those of the wind, wave and 1P (rotor frequency) and 3P (blade shadowing frequency) [6]. Typically a soft-stiff design where the structure's frequency is between 1P and 3P would be targeted. Nevertheless, this gap is very small, which may result in a design prone to dynamic amplification of responses [7]. This enhances the fatigue damage and reduces the intended design life [8]. Furthermore, bigger, more efficient turbines will help drive costs down 30% by 2020 [9], which will help offshore wind to compete with more conventional energy sources. An example of this is the recently upgraded V164-8.0 MW OWT, which enables an 8 MW platform to reach 9 MW depending on specific site conditions. It set a new record for power production at Østerild, generating 216,000 kWh over a 24 h period. Torben Hvid Larsen, MHI Vestas CTO stated that this OWT will play an integral part in enabling the OW industry to drive LCOE down.

A trade-off between durability of structures and the CAPEX costs needs to be made. Durability is the resistance to age-related deterioration, in particular corrosion and fatigue due to operational and environmental loads. Certain structures have less structural redundancy or may be inherently designed to resist higher stresses [10]. CAPEX is taken to mean an expenditure whose benefit extends beyond one year, and refers here to the costs associated with building and installing the plant. CAPEX mostly comprises material and labour costs for turbines, foundations, and inter-array cabling, but also includes construction financing, development costs, and operating capital [11]. According to [12], 32% and 14% of the CAPEX will be spent on turbine and foundation costs respectively, in offshore projects. Cost modelling of OWTs constitutes a broad field; however, it is safe to say that by bringing the cost of the turbine and foundation down and not posing additional difficulty in installation and manufacturing, CAPEX will decrease [13]. This reduction in CAPEX will have a positive impact in the LCOE, which represents the Key Performance Indicator (KPI) that allows offshore wind to be compared to other, more conventional, energy sources. Wind energy and its further growth is hindered by wind's intermittent nature. Moreover, increasing OW

generation influences the reliability of electric power grids. Thus, there is a demand for new technical units providing ancillary services. Non-dispatchable renewable energy sources can be balanced by energy storage devices [14]. Despite near future levels of curtailment and intermittency, will not exclusively refinance additional storage but can aid reducing offshore connection charges representing around 20% of total CAPEX costs [15]. The design and control of OWTs require in-depth analysis in order to ascertain their energy capabilities and operation boundaries.

Today, as offshore wind is considered to be a relatively mature technology, operators are progressively feeling more comfortable with it and are willing to balance structural risks with a CAPEX reduction. The use of design methods and standards, and their combination with high fidelity FEA modelling, is considered a powerful and cost effective tool in the design of offshore structures. This paper identifies key design parameters (KDPs) for the design and scale-up of OWT support structures and analyses the potential impact that the implementation of engineering design decisions in these KDPs, will suppose structurally and economically.

2. Design provisions and parametric modelling of offshore wind turbine monopile structures

2.1. Key design parameters of OWT support structures

The KDPs of OWT support structures are identified through analysis of the relationships among its structural behaviour and economic parameters. Main input data to the model comprise parameters related to the environmental and site conditions, mainly related to the wind, wave and hydrodynamic loads. These will influence the wind turbine's geometry and material properties, which constitute the KDPs of the model. These KDPs can be modified for cost optimisation, or scale-up the OWT support structure which, combined with the scale-up of the OWT's rotor size, can be used to capture more wind. The effects of wind turbine size on the aerodynamic characteristics of a rotor blade were examined by [16], using CFD simulation. KDPs directly affect the KPIs of the system such as LCOE (Levelised Cost of Electricity produced), capacity, availability, etc. For example, a minimum stiffness and thickness (KDPs) are necessary to meet structural integrity requirements, in order to operate at nominal capacity (KPI) [8,17–19].

Environmental conditions play an important role in the design of OWT support structures, and a detailed study needs to be conducted in order to assess wind speed ranges, turbulence level, main wind and wave directions and how the structure will behave under their different interactions. Mean water level also plays an important role as the hydrostatic pressure can contribute towards stabilising the structure but also can pose design complications when moving to deep waters.

Since foundations constitute the pillars that sustain the whole structure, site investigation is crucial. Soil layer composition, depth and material properties, such as their strength, together with the environmental conditions, will determine the necessary pile depth. Pile thickness will not only be influenced by the site conditions, but also by the environmental excitations that will strongly determine the dynamics of the structure.

Although for a given rotor and nacelle dimensions, the weight and thrust force (KDPs) cannot be optimised from a structural point of view, their efficiency (aerodynamics combined with pitch and yaw control mechanisms) will make an impact on the turbine's power production (KPI). Moreover, environmental conditions will also have an impact on this matter. Additionally, for optimised power production that accelerates the ROI, a minimum tower length needs to be reached. Tower length, diameter and thickness are connected to ensure that not only safety limits (Ultimate Limit State (ULS), Fatigue Limit State (FLS) and buckling) are maintained, but also that enough stiffness is achieved so that natural frequencies are within the safety limits (1P and 3P frequencies), ensuring no resonance occurs.

Furthermore, the TP is a crucial part that interconnects the tower and the MP. Its KDPs would be the diameter and thickness, which need to be compatible with those of the tower and foundation. Thus, the number, size and volume of stoppers, which are the contact point between the TP and the MP, will strongly depend on the load excitations. Moreover, these KDPs can also influence the modal frequencies of the structure and become a dangerous risk in the event of extreme loading, leading to the loss of one or more of these stoppers; therefore, the structural integrity of the unit will be strongly compromised. Lastly, the TP's length and the volume of the stoppers could be optimised in terms of stiffness, natural frequencies and mass. Mass reduction is an important aspect of WTs' design as it can strongly affect CAPEX and therefore the LCOE of a project. The soil-structure interaction constitutes an important aspect of OWT support structure design. Soil profile properties make an important impact on the foundation's KDPs, which will vary depending on the type of foundation employed. Diameter, thickness and length constitute the main KDPs of MP foundations. However, other KDPs, such as joints in jacket structures, flooded members and marine growth, among others, would have to be considered for other foundation types [20].

2.2. Geometry

This study analyses how different variations of the geometry can contribute to the scalability and CAPEX reduction of OWT support structures. The reference site is located in the North of the UK. The reference turbine used for this analysis consists of a 3.6MW Siemens turbine, connected to an 80 m tower, a transition piece (TP) and is sustained by a monopile (MP) foundation. The MP is 31 m long and is embedded 18 m into the soil and submerged 11 m into the ocean. Fig. 1a shows a schematic of the OWT support structure 3D model. The TP (Fig. 1b) is 24 m in length and joins together the MP and the tower. Six stoppers located in the internal surface of the TP, would allow it to rest on top of the MP. The GC, located between

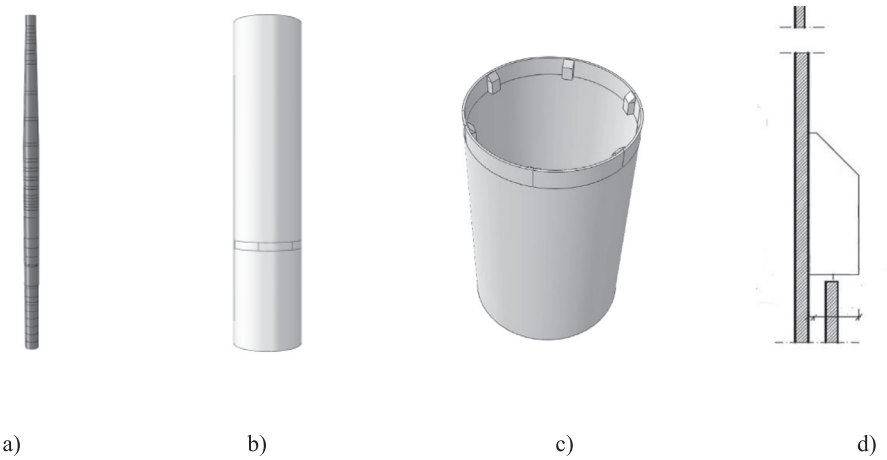

Fig. 1. a) Assembly of OWT support structure b) TP c) Stoppers within TP d) TP-GC-MP assembly.

the TP and the MP, is used for the appropriate transmission of loads and stresses. This assembly can be seen in Fig. 1c and d. The OWT support structure was modelled using Abaqus, which is a widely used FEA software.

2.3. Materials

2.3.1. Structural components

MP, TP, stoppers and the tower are made of steel S355 with a density of 7850 kg/m^3, a Young's modulus of 210 GPa, a Poisson's ratio of 0.3 and a nominal yield strength of 355 MPa. The GC's material properties are characterised by a density of 2740 kg/m^3, a Young's modulus of 88 GPa, a Poisson's ratio of 0.19 and friction coefficient of 0.6 [21].

2.3.2. Soil profile

Apart from the OWT support structure, an important part of the detailed parametric model is composed by the soil-structure interaction, which is a design factor of critical importance for the structural response of the pile-monopile-tower assembly. Paradoxically, the soil-structure interaction is an aspect often not considered in OWT support structures modelling [20]. The soil profile considered in this analysis consists of one layer of sand and three layers of clay. Composition of soil profiles strongly depends on the geographical emplacement; the soil profile utilised in this analysis corresponds to that of the North West of the UK. Table 1 shows the profile's soil parameters used in the simulations, which are based on site measurements. Winkler's approach was used to represent the soil profile. This method is widely used to model the soil-structure interaction by replacing the elastic soil medium with closely spaced and independent elastic springs [22,23]. Furthermore, it is recommended by DNV-GL [8], where the stiffness of the linear springs used in the Winkler's approach, is calculated from the p-y curves [24]. This method is used for the design of horizontal loaded piles by the American Petroleum Institute (API) code [17], and calculates the lateral soil resistance (p) as a function of lateral soil displacement (y). This empirical method is based on test results of laterally loaded piles and depends on the pile diameter, soil strength and loading conditions, although other factors such as layered soils or the space between piles have considerable influence [25,26].where γ' is the submerged unit weight, S_u is the undrained shear strength, δ is the characteristic interface friction angle, ϕ is the characteristic angle of internal friction, E is the Young's modulus, ε_{50} is the strain which occurs at one-half of the maximum stress in the laboratory undrained compression test, t_c is the unit skin friction under compression, t_t is the unit skin friction under tension and q is the unit tip resistance under compression.

Table 1
Soil properties based on site measurements.

Depth (m)		ɣ' KN/m^3	S_u kPa	δ deg	ϕ deg	E MPa	ε_{50} (%)	t_c kPa	t_t kPa	q (MPa)
SAND	2.4	11	0	37	42	22.7	0	8	8	1.1
	5.4	11	0	37	42	33.3	0	25.9	25.9	3.7
	8.0	11	0	37	42	44.3	0	44.4	44.4	6.3
CLAY	8.4	10	750	0	0	300	0.2	220.7	220.7	6.8
	11.0	10	750	0	0	300	0.2	229.1	229.1	6.8
	13.0	10	575	0	0	230	0.2	198.0	198.0	5.2
	18.0	10	800	0	0	320	0.1	273.1	273.1	7.2

Although this approach is widely used and recommended in design standards, it was developed for up to 2 m diameter piles [27]. Therefore, pile deformations might be underestimated [28]. Although a cyclic version of the p-y curve was introduced in [29], it is neither cycle nor amplitude dependent, and provides only a lower bound on the soil-pile lateral stiffness. This shortcoming is overcome in [30] by the utilisation of the quasi-static p-y degradation model of [31]. Continuum modelling of the soil in an FE analysis constitutes a different approach, where the soil is modelled as a large volume. This approach is more accurate when dynamic studies are carried out; however, it also requires significantly more computational resources. Therefore, for the iterative process required for this paper, a more computationally intensive approach was considered beyond the scope of the aims set to this publication. Besides, as steel is an elastic material, the relationship between its stresses and deformations is linear, making Winkler's approach accurate enough for the purpose of this study.

2.4. Mesh sensitivity analysis

A mesh sensitivity analysis was performed in order keep a balance between the computational time of the simulations and the accuracy of the results. In the process, it was found that the structure's eigenfrequencies were especially sensitive to the size of the mesh. After the analysis, a mesh size of 0.1 m was found to be adequately accurate as results had already converged. This mesh size will therefore save unnecessary computational time in comparison to a further mesh refinement of 0.05 m.

2.5. Validation

This model has been validated by comparing the results of the modal analysis of both the structure and the tower, against data from the reference OWT. Among these data, it was specified that the eigenfrequencies of the system and the tower must be within the range of 0.275–0.320 Hz and around 0.506 Hz respectively. Results of the modal analysis can be seen in Table 2, where it can be appreciated that the first eigenfrequency of the model is within this range that typically represents the 3P frequency of the rotor. Moreover, the eigenfrequency of the tower is 0.533 Hz, which represents a 5.3% of relative difference from the one suggested by the manufacturer. This difference is considered to be acceptable as internal platforms and secondary steel assets have not been included in the simulation.

3. Load calculations for offshore wind turbine support structures

The design's environmental conditions approach followed in this study, is based on the use of the highest extreme conditions likely to occur in a return period of 50 years [32,33] for ULS and buckling limit states and normal operating conditions for the FLS limit state, which are introduced in Section 4. Wind, wave and current loads are manually calculated under this premise and then introduced in the FEA parametric model. Although many load cases need to be considered for the design, according to the above mentioned standards, the structure needs to be able to withstand the simultaneous combination of these three loads, acting in the same direction, which is considered the worst static load case scenario.

3.1. Wind

For representation of wind climate, a distinction is made between normal and extreme wind conditions. The former generally concern cyclic structural loading conditions, which are important for fatigue assessment, while the latter are wind conditions that can lead to extreme loads, which might lead to the collapse of the structure due to excessive loading. Accurate estimation of the occurrence of extreme wind speeds is an important factor in achieving an affordable level of risk and balance between safety considerations and "over-design" of the structure [34]. Both normal and extreme wind conditions used in this analysis were calculated in accordance with IEC 61400-1 [32], and are summarised in Table 3.

Calculating wind loads along the structure can be done applying the following formula:

$$V(h) = V_{ref} * \frac{ln\left(\frac{h}{z_0}\right)}{ln\left(\frac{h_{ref}}{z_0}\right)} \tag{1}$$

where z_0 is the roughness coefficient, which can be taken from [8]. Once the wind speed profile has been generated, the force in the horizontal direction affecting the tower, TP and nacelle, produced by the wind can be calculated as:

Table 2
Validation of eigenfrequencies. System and Tower.

	FEA Model	Real Data
Tower	0.533 Hz	0.506 Hz
System	0.291 Hz	0.275–0.320 Hz

Table 3
Normal and extreme wind parameters.

Subject	Issue	Unit	Value
Normal Conditions	Mean air density, ρ	kg/m^3	1.23
	Mean wind speed (80 m), V_{ave}	m/s	8.4
	Maximum flow inclination	deg	0
Extreme Conditions	Air density at extreme wind, ρ_e	kg/m^3	1.225
	Maximum wind speed at hub height, V_{max}	m/s	45.2

$$F_x = \frac{1}{2} * C_D * \rho_e * (V_{max})^2 * A * \cos\alpha \quad (2)$$

where:
C_D = drag coefficient of a cylinder in the case of the tower and TP and a plate in the case of the nacelle. Blades are not taken into consideration in this study.
A = area being pushed by the wind.
α = inclination angle of the wind with the horizontal axis

3.2. Wave

Wave loading is another environmental load that influences the structural integrity of OWT support structures. Wave forces are calculated using Morrison's Equation, which is composed of two terms, representing the inertia and drag [35]. These terms can be identified by the inertia and drag coefficients (C_m and C_D respectively). Morrison's Equation can be expressed as:

$$F = \frac{1}{2}\rho C_D D|U|U + C_m \rho \frac{\pi D^2}{4}\frac{dU}{dt} \quad (3)$$

where:
U = undisturbed fluid velocity
$\frac{dU}{dt}$ = acceleration of the fluid
ρ = water density
D = diameter of the cylinder

As explained at the beginning of this section, the design wave approach is based on the use of the highest wave likely to occur in a given return period (50 years in this case). Waves are characterised in terms of height (H) and wave period (T). These parameters are summarised in Table 4 and were estimated at the offshore emplacement where the turbine is installed in the North of the UK.where H_s is the significant wave height, H_{max} is the maximum wave height, T_z is the zero up-crossing period and T_{peak} is the peak-to peak-period.

In order to calculate the wave's velocity and acceleration, linear wave theory for shallow water was employed. Airy wave theory was developed by the mathematician and astronomer G.B. Airy in 1845. This wave theory is summarised in the Airy velocity potential formula:

$$\Phi(x, y, t) = -ac\frac{\cosh k(y+d)}{\sinh(k+d)}\cos(kx - wt) \quad (4)$$

where:
a = amplitude (m)
c = celerity (m/s)
k = wave number
d = depth
x, y = horizontal and vertical coordinates
w = wave frequency
t = time

Table 4
Summary of extreme metocean conditions.

Return period (years)	Water level LAT (m)	Hs (m)	Hmax (m)	Tz (s)	Tpeak (s)
1	10.05	4.90	9.2	9.8	13.5
10	10.48	5.90	11.0	11.5	14.8
50	10.93	6.60	12.1	12.7	15.5

From the Airy velocity potential, the fluid's velocity ($U(x,t)$) and acceleration ($\dot{U}(x,t)$) in shallow waters can easily be calculated as:

$$U(x,t) = \frac{\partial \Phi(x,y,t)}{\partial x} = \frac{wa}{kd}\sin(wt - kx) \tag{5}$$

$$\dot{U}(x,t) = \frac{dU(x,t)}{dt} = \frac{w^2 a}{kd}\cos(wt - kx) \tag{6}$$

After the fluid's velocity and acceleration are calculated, the wave loads can be calculated from Morrison's Equation. Mass and drag coefficients, C_m and $C_{D,}$ are usually estimated according to the offshore standards [8] by firstly, deriving the drag coefficient for steady-state flow (C_{DS}) from Eq. (7), then reading off the wake amplification factor ($\psi(K_c/C_{DS})$), which depends on the Keulegan-Carpenter number (K_c) and C_{DS} and calculating C_D and C_m from Eqs. (10) and (11) [36].

$$C_{DS} = \begin{cases} 0.65 & for\ k/D < 10^{-4} \quad (smooth) \\ \frac{29+4\log_{10}(k/D)}{20} & for 10^{-4} < k/D < 10^{-2} \\ 1.05 & for\ k/D > 10^{-2} \quad (rough) \end{cases} \tag{7}$$

$$K_c = \frac{U_{max} T_p}{D} = 17.7 \tag{8}$$

$$\Psi\left(\frac{K_c}{C_{DS}}\right) = 1.2 \quad \text{from[36]} \tag{9}$$

$$C_D = C_{DS}{}^{*}\Psi\left(\frac{K_c}{C_{DS}}\right) = 0.78 \tag{10}$$

$$C_m = \max\{2.0 - 0.044(K_c - 3); 1.6 - (C_{DS} - 0.65)\} = 1.6 \tag{11}$$

3.3. Tidal and current induced loads

Tidal currents and wind driven currents are two environmental loads that even though they do not represent major hazards to the structure's integrity in shallow waters, they contribute to other major excitations such as those produced by the wind and waves. The tidal current profile can be represented as the current speed ($v(z)$) at distance z, from still water level (positive upwards), which is the exponential variation of the current at still water level v_0 through the distance to the top of the water column z.

$$v(z) = v_0\left(\frac{h+z}{h}\right)^{\frac{1}{7}} \quad for\ z \leqslant 0 \tag{12}$$

where h is the water depth.

The extreme tidal current takes place approximately at mean water level, with zero tidal current at high and low tide. Once the tidal current profile is calculated, it will be modelled as a constant over depth current. Wind driven currents are due to wind imposed shear forces on the water surface and are, therefore, likely to be oriented in the same direction as the wind. The wind driven current at the sea surface is estimated in accordance with IEC61400-3 [33], as:

$$U_{wind} \approx 0.01 U_{1h,10min} \tag{13}$$

where $U_{1h,10min}$ is the hourly mean at 10 m height.

3.4. Hydrostatic pressure

Hydrostatic pressure is referred to as the pressure of the water column applied to the submerged parts of the MP and TP. It can be calculated from a control volume analysis of an infinitesimally small cube of fluid and simplified, as density and gravity are constant through depth.

$$p(z) - p(z_0) = \frac{1}{A}\int_{z_0}^{z} dz' \int\int^{\rho} (z')g(z')dA = \int_{z_0}^{z} dz'\rho(z')g(z') = \rho g h \tag{14}$$

where:

$p(z)$ = pressure at a given height z

$p(z_0)$ = pressure at z_0, which is the top of the water column

Therefore $p(z_0) = p_{atm}$

ρ = water density (kg/m^3)
g = gravity (m/s^2)
$h = (z - z_0)$ = height of the liquid column between the test volume and the zero reference point of the pressure

3.5. Nacelle's and rotor's weight

Since the nacelle's and rotor's (composed of the hub and blades) detailed modelling is not part of the parametric model, they are included in the FEA as concentrated or distributed masses in order to be able to reproduce accurately the OWT's structural behaviour. According to [37], there is no need to model the blades due to the fact that, aside from the mass added to the tower top, parked and feathered blades have minimal impact on the natural frequency of OWTs. The nacelle's and rotor's weights are 125 and 95 tons respectively, which makes a total of 220 tons that are accounted as a cylinder three metres high and with the same diameter as the top of the tower. The density was increased accordingly in order to account for the total weight. The nacelle's and rotor's weights were found in the official Siemens SWT-107 3.6 MW brochure [38].

4. Limit states formulation

Structural integrity of the system is checked according to DNV-OS-J101 [8], which is the most widely used standard in the design of OWTs. According to this standard, four limit states have to be considered in the design: ULS, FLS, Accidental Limit State (ALS) and Serviceability Limit State (SLS). The modifications in the design carried out in the design cases considered were checked upon ULS and FLS. ALS was not considered as this limit state is used for the assessment of structural damage in the structure, caused by accidental loads or to re-assess the ultimate resistance and structural integrity after damage. Similarly, SLS was not taken into account as it considers tolerance criteria applicable to normal use of the OWT support structures. Furthermore, the structural performance of the system was also checked upon buckling and natural frequencies.

4.1. ULS

ULS analysis is carried out considering extreme environmental conditions the worst case scenario for a 50 year return period. This is when wind, wave, tides and wind driven currents are aligned in the principal direction of the wind (SW). The load factor to be used when different loads are combined to form the design load is 1.35 [8]. This load factor is also applicable in operational loading; however, as an extreme loading case is being considered, the turbine cannot be operating due to safety reasons. Therefore, parked conditions apply.

In Section 3, extreme loads were calculated with a load factor of 1.35. From the combination of these loads, the utilisation factors are derived. Table 5 shows the Maximum Utilisation Rates (MUR) and therefore the Maximum Stresses Allowed (MSA) for the MP and the TP in the baseline case, which will be use to assess the loss or gain of the structural integrity of the different design cases considered. MUR and MSA are related by the following expression:

$$MUR(\%) = \frac{MSA}{\sigma_{yield}} * 100 \tag{15}$$

4.2. FLS

FLS refers to the cumulative damage in the structure due to cyclic loads. The fatigue design of OWT support structures is governed by dynamic responses from simultaneous aerodynamic and hydrodynamic loads [39]. The structure must be able to resist expected fatigue loads, which may occur during temporary and operational design conditions. The load factor in the FLS is 1.0 for all load categories [8]. Normal sea state conditions (significant wave height and peak spectral period) were used for the calculation of wave loading [33]. Wind loads were taken from [40], where the fatigue thrust load for the tower of a 3.6 MW OWT with 100 m hub height are 143kN.

The two most commonly used fatigue assessment techniques are the stress life (S–N) approach and the fracture mechanics approach. The S–N curve approach is the one recommended by standards [8] and [33]. A review of the currently used S–N curves is provided in [41]. Furthermore, the equivalent stress range ΔS can be determined from the parametric FEA model subjected to the previously mentioned fatigue loads. Having obtained the equivalent stress range, the number of loading cycles to crack initiation, in Eq. (15), can then be determined from the S–N curve, expressed as:

Table 5
Maximum utilisation rate for MP and TP in the baseline case.

MP		TP	
MUR (%)	MSA (MPa)	MUR (%)	MSA (MPa)
68	227.8	52	174.2

$$\log N = A - m \log \Delta S \tag{15}$$

where A is the intercept, m is the slope of the S–N curve in the log–log plot.

The selection of the S–N curve plays a massive role in the results obtained. These are generally classified in: air, seawater with adequate cathodic protection or free corrosion conditions, and are taken from DNV-RP-C203 "Fatigue Strength Analyses of Offshore Steel Structures" [42]. Offshore structures are prone to corrosion development due to the harsh marine environment, which leads to significant levels of damage to the structures and hence a reduction in service life [43]. For that reason, curve D in seawater with adequate cathodic protection is used in service life calculations.

4.3. Buckling

Buckling is a failure mechanism, to which slender structures are prone. It is caused by a bifurcation of static equilibrium equations solution [44]. Buckling is characterised by the sudden failure of a structural member subjected to high compressive stress. During this phenomenon, the compressive stress at the point of failure is less than the ultimate compressive stress of the material. When the applied load is increased on a slender structure, such as a column, there is the possibility that it becomes large enough to cause the structure to lose its stability and buckle. Any further load will cause significant and somewhat unpredictable deformations, possibly leading to complete loss of the member's load-carrying capacity.

Eigenvalue linear buckling analysis is generally used to estimate the critical buckling load of the analysed structure. The buckling loads are calculated relative to the base state of the structure, which can include preloads (e.g., bolt preload). In an eigenvalue buckling problem we search for the loads for which the model stiffness matrix becomes singular, so that the problem has non-trivial solutions [45]. The buckling stability of shell structures is often checked according to DNV-RP-C202 [18] or Eurocode 3/ EN 1993-1-1 [46] and Eurocode 3/ EN 1993-1-6 [47]; in this analysis Abaqus CAE is used to assess it.

4.4. Natural frequencies

Resonance is a phenomenon in which a vibrating system or external forces (in this case environmental and operational loads experienced by the OWT support structure) drive another system to oscillate with greater amplitude at a specific preferential frequency. These amplified oscillations produce higher than expected deformations, a rise in stress within different parts of the turbine, which will lead to crack initiation, and generally a decrease in the fatigue life of the structure. Furthermore, the fact that wave loading and the turbine's operating loads are cyclic loads, makes the design of these structures particularly difficult.

A classic aspect of good structural design lies in optimizing stiffness-to-mass ratio through material and shape choices. Natural frequencies' sensitivity analyses are carried out for the different case studies with the aim of detecting patterns of change in the characteristic natural frequencies of the structure that could potentially be employed for its scale-up or to monitor a particular failure mechanism.

Modal frequencies monitoring is a common structural health monitoring technique implemented in OWTs that identifies their modal frequencies whose deviations are a damage symptom [48]. This is carried out by the installation of accelerometers either in the nacelle of the turbine or along the tower and support structure. However, because the wind and wave loading applied to the structure cannot be measured accurately in a continuous manner, Operational Modal Analysis (OMA) needs to be employed. This technique allows identification of the resonance frequencies every 10 min without any human interaction [49] based on the assumption that the structure is subjected to unknown random loads [50,51]

5. Sensitivity analysis and results

In Section 2.1, a number of KDPs of OWT support structures were identified. In this section, three KDPs have been chosen based on their preliminary capacity of impacting on the design of OWT support structures in terms of scaling-up and CAPEX reduction. The cases considered in this study are: TP's and GC's length, effect of size and number of stoppers, and scour development.

5.1. Design Case A: TP's and GC's length

Case study A checks the sensitivity of the length of the TP and GC, which comprises from where the stoppers are assembled, to the bottom of the TP. The grout, not only enhances the correct transmission of loads and stresses from the TP to the MP, but also contributes to the accurate positioning of the two components. In the baseline turbine this length is 7.8 m. Variations of one and two metres have both been added and subtracted from this baseline length of 7.8 m to complete the analysis.

Depending on the variation in the natural frequencies of the OWT, once it has been scaled-up to a bigger turbine, modifications to its geometry can be applied to intentionally increase or decrease the turbine's natural frequency. Furthermore, savings or additions in material will make an economic impact on the CAPEX, as the cost of materials is an important driver [11–13]. To that aim, sensitivity analyses of natural frequencies, ULS, FLS and buckling checks have also been carried out. The

benefit of these checks is not only to scale-up the turbine (ensuring the health of the structure), but also to potentially save a considerable amount of material and therefore money.

Table 6 shows the variation in the first six natural frequencies. From this sensitivity analysis it can be appreciated that the variation of the first two natural frequencies, which are those that are dangerously close to the 1P and 3P rotor frequencies, is low. This suggests that reducing the TP's and GC's length will not necessarily enhance scalability, as natural frequencies change at a low rate. However, this brings up the possibility of saving materials and therefore reduce CAPEX. In order to be able to do that, ULS, FLS and buckling checks will have to support this reduction in length.

Tables 7 and 8 present the results from the ULS and buckling checks, being the buckling frequency for a particular load combination, the inverse of the utilisation factor for the structure to buckle. Table 7 shows that no major changes in the MUR occur due to this length variation. Moreover, buckling frequency does not change due to this length reduction, although it has a slight tendency to decrease when the length of the TP is increased. These results show in the case of the TP length reduction (5.8 m and 6.8 m), that because of the decrease in the weight of material, an increase in the buckling frequency could be expected. The lack of variation in results suggests that this reduction must have been compensated by a loss of support produced by a reduction of the GC length.Table 9

The FLS check shows no rise in the effective stress range (ΔS), when the TP's and GC's lengths are reduced. This indicates that fatigue life will be maintained and therefore, as ULS and buckling checks also allowed it, almost 20 tons of material could be saved and therefore material costs will be reduced.

5.2. Design Case B: Effect of size and number of stoppers

Case study B evaluates the effect of adding or suppressing stoppers in the integrity of the structure and its natural frequencies. The six stoppers of the reference turbine were increased to eight and 12 and then decreased to four. The volume of steel utilised in the stoppers is continuous, therefore modification in the number of stoppers necessarily implies a variation in the stopper dimensions. This assumption implies that no cost in materials will be added or saved and the results will just impact on the integrity of the structure. Table 10 shows the stoppers' dimensions. As can be observed below, the dimensions of the stopper's base (B2) have been maintained in all cases. This is due to the fact that the relative position between the TP and the MP does not change throughout Design Case B.

From the frequencies' sensitivity analysis (Table 11), the large variation that the number and distribution of stoppers produces in the natural frequencies can be observed. A dramatic drop in the natural frequencies occurs when just four stoppers are used, making the first two frequencies fall into the boundaries of resonance with the rotor frequencies. In the case of eight stoppers, a slight drop also occurs, although not as severe as for the four stoppers. This sensitivity analysis shows that

Table 6
Case A: Percentage of variation of modal frequencies.

Modal frequencies	Transition Piece Length				
	5.8 m	6.8 m	7.8 m	8.8 m	9.8 m
1	−1.01%	−0.52%	0.29089 Hz	0.54%	1.10%
2	−1.05%	−0.54%	0.29615 Hz	7.41%	7.75%
3	0.84%	0.39%	1.6776 Hz	−0.35%	−0.65%
4	0.77%	0.36%	1.7211 Hz	−7.30%	−7.90%
5	−1.17%	−0.53%	1.9516 Hz	0.41%	0.75%
6	−1.11%	−0.50%	2.0637 Hz	0.40%	0.71%

Table 7
Case A: ULS check: MURs (%) of the OWT support structure.

MUR (%)	Transition Piece's Length				
	5.8 m	6.8 m	7.8 m	8.8 m	9.8 m
MP	64.72%	64.73%	64.73%	64.72%	64.70%
TP	21.84%	22.17%	22.39%	22.60%	22.76%

Table 8
Case A: buckling check.

Buckling frequency (Hz)	Transition Piece's Length				
	5.8 m	6.8 m	7.8 m	8.8 m	9.8 m
	1.5316	1.5316	1.5316	1.5291	1.5296

Table 9
Case A: FLS analysis.

Transition Piece's Length					
TP length	5.8 m	6.8 m	7.8 m	8.8 m	9.8 m
ΔS(MPa)	33.9	33.9	33.9	34.5	35.0
Fatigue life (yr)	32.9	33.0	33.1	29.9	28.1

Table 10
Stopper's dimensions keeping a constant volume of steel.

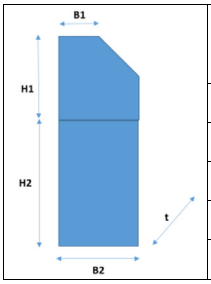

Dimension (m)	Number of Stoppers			
	4	6	8	12
B1	0.02	0.02	0.02	0.02
B2	0.21	0.21	0.21	0.21
H1	0.20	0.18	0.17	0.15
t	0.407	0.316	0.290	0.260
H2	0.50	0.42	0.33	0.23

Table 11
Case B: sensitivity analysis of modal frequencies.

Case B: Stopper Configuration				
Mode	4 Stoppers	6 Stoppers	8 Stoppers	12 Stoppers
1	−17.11%	0.29089 Hz	−1.54%	0.11%
2	−17.61%	0.29615 Hz	−0.93%	0.11%
3	−5.07	1.6776 Hz	−2.24	0.12%
4	−5.18%	1.7211 Hz	−1.53%	0.12%
5	−5.38%	1.9516 Hz	0.16%	0.16%
6	−5.56%	2.0637 Hz	0.38%	0.38%

Table 12
Case B: buckling analysis.

Buckling frequency (Hz)	4 Stoppers	6 Stoppers	8 Stoppers	12 Stoppers
	1.12	1.53	1.55	1.50

the distribution of stoppers every 90 and 45 degrees produces a drop in natural frequencies, as opposed to 60 and 30 degrees distribution, as these frequencies are higher for a TP with six and 12 stoppers than for four and eight.

From the buckling analysis (Table 12) it is clear that the four stopper distribution is not a safe alternative, due not only to its first two natural frequencies being very close to resonance, but also to the moderate reduction of the buckling frequency from 1.53 Hz to 1.12 Hz, which means that for the same amount of material being spent in the stoppers, the OWT support structure can take 1.12 times the extreme loads instead of 1.53 times. This will compromise the integrity of the structure. Furthermore, buckling would take place between the TP and MP, which is not the case in the six, eight and 12 stopper distributions. The eight stopper distribution slightly improves the buckling capacity, which is marginally reduced in the 12 stopper distribution. Nevertheless, this reduction is within reasonable limits that do not threaten the integrity of the structure.

Results of the ULS analysis are summarised in Table 13. The four stopper distribution is again characterised by bad results, showing much higher MURs than the six stopper configuration, which are very close to the yielding point of the steel and therefore, not safe. The eight and 12 stopper configurations appear to considerably improve the MURs for both the MP and the TP.

In the fatigue check, the four stopper configuration presents similar results to the other structural checks performed, with an increase in ΔS of 42.5%, which makes a considerable reduction in service life. Other configurations results, shown in Table 14, present a non-existent or very low rise (1.8%) in ΔS of the eight and 12 stopper configurations, in comparison to the six stopper's, respectively.

Table 13
Case B: ULS check: MURs (%) of the OWT support structure.

MUR (%)	Stopper Configuration			
	4 Stoppers	6 Stoppers	8 Stoppers	12 Stoppers
MP	81.42%	64.73%	58.54%	54.57%
TP	96.99%	22.39%	8.67%	8.86%

Table 14
Case B: FLS analysis.

Stopper Configuration				
No. of stoppers	4 Stoppers	6 Stoppers	8 Stoppers	12 Stoppers
ΔS(MPa)	48.3	33.9	33.9	34.5
Service life (yr)	5.6	33.1	32.8	30.2

Table 15
Case C: sensitivity analysis of modal frequencies.

Case C: Scour Development				
Mode	No Scour	1 m Scour	2 m Scour	3 m Scour
1	0.29037 Hz	0.00%	0.00%	0.00%
2	0.29594 Hz	−0.42%	−0.74%	−0.97%
3	1.6755 Hz	0.00%	0.00%	0.00%
4	1.7203 Hz	−0.57%	−1.02%	1.34%
5	1.9519 Hz	0.00%	−0.01%	−0.02%
6	2.0642 Hz	0.00%	0.00%	0.00%

5.3. Design Case C: scour development

Case study C assesses the effect that scour development has not only on the natural frequencies of the structure, but also on its integrity. Scour is one of the biggest issues currently being faced by operators. This phenomenon occurs around the foundations of structures when these are placed into a marine environment and exposed to water currents and tides. Due to the presence of the structure itself, different changes affect the natural flow regime at the sea bed around the foundation, which lead to increased sediment mobility [52]. Depending on the foundation type and the environmental conditions, scour depths of several metres around the OWT support structure could be observed even within short periods [53].

Rambabu et al. [54] stated that the fluid flow, geometry of foundation and seabed conditions are the governing factors for seabed scouring. The characteristics of fluid flow include the current velocity, Reynolds number of the model and Froude number of the flow. Therefore, for different foundation types, different scouring patterns will develop [55]. The scour development around MP structures has been studied extensively for the foundation of OWT in the past few decades [56].

This design case was selected in order to make a structural analysis of how the whole OWT support structure will be affected by scour development. This FEA model includes not only the tower of the OWT, which is the common focus of FEA modelling [57–61]; but also the support structure and MP-soil interaction with multi-layered soil composed of layers of both clay and sand, which is not present in most of the studies, due to the difficulty of modelling sand layers [28,62,63]. However, this analysis does not take into account the process or the mechanism of the scour development, as it is considered beyond the scope of this study. Therefore, the structural analysis carried out in this publication assumes the scour has already developed. These analyses were carried out by recalculating the value of the springs' stiffness used to model the soil, assuming that the first one, two and three metres of soil had disappeared due to the scour process.

From previous research, a significant impact on the structure's integrity was anticipated because as scour develops, a lesser percentage of the MP is embedded in the soil, producing eigenfrequency reductions and therefore, leading to resonance. Table 15 corroborates this prediction; however, surprisingly, not for the first natural frequency. As can be observed, changes in the natural frequencies occur mainly in the second and fourth modes. Because the first and the second natural frequencies are very close to each other, the fact that there is significant variation in the second mode still poses a threat to the structure.

It seemed reasonable to believe that as scour develops, the MP's MUR would increase, due to the loss of support from the soil. However, results do not show significant changes in MURs (Table 16), which remain practically unaltered. Furthermore, the more the scour is developed, the lower buckling capacity the OWT support structure presents (Table 17), which could become a threat to its integrity if the process continues, although the capacity remains within safety limits in this design case.

Furthermore, Table 18 shows how scour development increases the stress range, making the service life of the OWT support structure shorter. It is also worth bearing in mind that particular soil types with low cohesion will be more prone to

Table 16
Case C: ULS check: MURs (%) of the OWT support structure.

MUR (%)	Scour Development			
	No Scour	1 m Scour	2 m Scour	3 m Scour
MP	64.73%	64.74%	64.75%	64.76%
TP	22.39%	22.43%	22.43%	22.43%

Table 17
Case C: buckling analysis.

Buckling frequency (Hz)	No Scour	1 m Scour	2 m Scour	3 m Scour
	1.53	1.51	1.46	1.43

Table 18
Case C: FLS analysis.

Scour Development				
Level of Scour	No Scour	1 m Scour	2 m Scour	3 m Scour
ΔS(MPa)	33.9	36.5	37.7	41.9
Service life (yr)	33.1	22.7	19.3	11.4

scour development, which can be a quick phenomenon if it is not mitigated. Furthermore, given the moderate rate of change (7.7%, 11.2% and 23.6% in 1 m, 2 m and 3 m scour respectively) of the stress range that scour produces, special effort should be put either into frequent and costly inspections, or into scour mitigation and prevention measures. Additionally, it is recommended to take account of the scour development into the reliability assessment of OWT support structures, providing more accurate reliability assessment results for reliability-based inspection of OWT support structures.

6. Discussion

Case A was proved to be effective in materials cost reduction but not in modal frequencies control. The reduction in length of the TP and GC of the OWT support structure produced low variation in modal frequencies, which will be reduced within safety limits. Furthermore, as ULS, FLS and buckling are not compromised by these modifications, a lower safety factor could be employed in the future for TP and GC design, reducing their length. As a consequence, material costs could be reduced, as more than 20 tons of steel could be removed per turbine.

No material reduction is allowed in Case B due to the constant volume of steel employed in the stoppers. However, the interest in this case study remains in its potential to decrease the fatigue damage and to improve the buckling capacity and MUR of the OWT support structure just by changing the number (and therefore the dimensions) of the stoppers and their distribution. Within this case study, it was proved that the distribution of the stoppers plays an important role in the structural integrity of the unit. Besides the fact that the four stopper distribution was not structurally safe in terms of natural frequency, stability, buckling capacity and fatigue life, results show that eight stopper distribution produces a minor decrease in natural frequencies (between 0.1% and 1.5% depending on the mode), and a moderate and major decrease in the MP's and TP's MUR (9.6% and 86% respectively). Furthermore, the stress range remains almost equal to the baseline's. These results show that, although the eight stopper configuration fails in the enhancement of fatigue life, it has a very positive effect on the structure's behaviour against extreme loads.

Although the results for the 12 stopper distribution are generally good, (minor rise (between 0.1% and 0.4%) in natural frequencies, minor reduction in buckling capacity without safety repercussion and great improvement (15.7% and 86% respectively) in the MP's and TP's MURs, the cost of installation (welding to the TP) will inevitably be higher and take longer to be completed. Therefore, special consideration of this rise in costs and the benefits to the turbine's structural integrity, will have to be considered. Furthermore, FLS results present a slight increase in the stress range, which leads to a reduction in the service life from 33.1 years to 30.2 years.

Case C highlights the importance of scour monitoring and the impact that its development can have on the structure's integrity [64]. From the natural frequencies' sensitivity analysis it can be concluded that, although the first mode does not present variation due to scour, modes two and four could potentially be used to detect the development of this phenomenon. The behaviour of the structure against extreme loading is not compromised due to scour development, presenting a minimal increase in the MP's and TP's MURs. A remarkable reduction of 6.5% in the buckling capacity takes place when the scour reaches 3 m. Furthermore, given the moderately high rate of change (7.7%, 11.2% and 23.6% in 1 m, 2 m and 3 m scour respectively) of the stress range and therefore expected service life (from 33.1 to 22.7, 19.3 and 11.4 years, respectively) that

scour produces, special effort should be put either into frequent and costly inspections, or into scour mitigation and prevention measures.

The design of scour protection should be integrated into the foundations' design [65]. In order to carry out an effective design, sediment properties, seabed's geotechnical composition, environmental conditions and turbine specifications, among others, have to be taken into account and must accurately predict the maximum scour that would occur in the absence of this protection [66].

7. Conclusions

A good understanding of how geometrical modifications to the structure will affect its structural integrity and end of life is vital to adapt these structures to harsher environments further from shore [67]. To this end, a sensitivity analysis of three KDPs of OWT support structures was carried out, in order to analyse whether these KDPs could contribute to the turbine's scale–up by either modifying its modal properties, improving structural integrity, or saving in CAPEX. Three case studies were considered for this analysis: Case A: reduction of the TP's and GC's length, Case B: stoppers optimisation and Case C: scour development. The following conclusions can be drawn from the present study:

- A reduction in the TP's and GC's length was proven to maintain the structure's integrity within safety limits. Therefore, although reducing the TP and GC's length will not necessarily enhance their scaling-up, due to the minimal change in natural frequencies, it will save almost 20 tons of steel per turbine. This measure will provide a considerable reduction in CAPEX, when applied to all the units within a WF.
- Increasing the number of stoppers while maintaining the volume of steel, was proven to have a positive impact on the structure's integrity for both the eight and the 12 stopper configurations. However, as cost of installation (welding the stoppers to the TP) will inevitably be higher and take longer to be completed, special consideration of the trade-off between this rise in costs and the benefits to the structural integrity, will have to be made. The eight stopper configuration may constitute a good compromise between the six and 12 stopper configurations without reducing the expected service life of the structure.
- Scour is one of the biggest issues currently being faced by operators, which was proven to compromise the buckling capacity and fatigue life of OWT support structures. Modes two and four showed special sensitivity to the development of this phenomenon. For that reason it is believed that Integrity Monitoring could become a good alternative to monitor them in order to detect and control this phenomenon. However, before the installation of the instrumentation, no overlapping between failure mechanisms, that would also affect modal properties, must be ensured in order to avoid misleading information about the threat and its extent at that particular time.

Acknowledgements

This work was supported by grant EP/L016303/1 for Cranfield University, Centre for Doctoral Training in Renewable Energy Marine Structures (REMS) (http://www.rems-cdt.ac.uk/) from the UK Engineering and Physical Sciences Research Council (EPSRC) and Innogy SE.

References

[1] RenewableUK, Wind Energy in the UK. State of the Industry Report Summary 2015, (2015) 1–43. http://www.renewableuk.com/en/publications/guides.cfm.
[2] Energy Technologies Institute, Options, Choices. Actions, UK Scenarios for a low carbon energy system transition, 2015.
[3] Carbon Trust, Floating Offshore Wind : Market and Technology Review, 2015. http://www.carbontrust.com/media/670664/floating-offshore-wind-market-technology-review.pdf.
[4] EWEA Business Intelligence, Aiming high: Rewarding Ambition in Wind Energy, n.d. doi:10.1021/nn700402d.
[5] A. Ho, A. Mbistrova, G. Corbetta, EWEA. The European Offshore Wind Industry: Key Trends and Statistics 2015, European Wind Energy Association, n.d. http://www.ewea.org/fileadmin/files/library/publications/statistics/EWEA-European-Offshore-Statistics-2014.pdf.
[6] S. Bhattacharya, Challenges in design of foundations for offshore wind turbines, IET Eng. Technol. Ref. (2014) 1–9, http://dx.doi.org/10.1049/etr.2014.0041.
[7] M. Damgaard, V. Zania, L.V. Andersen, L.B. Ibsen, Effects of soil-structure interaction on real time dynamic response of offshore wind turbines on monopiles, Eng. Struct. 75 (2014), http://dx.doi.org/10.1016/j.engstruct.2014.06.006.
[8] DNV (Det Norske Veritas), DNV-OS-J101 Design of Offshore Wind Turbine Structures, 2014.
[9] RenewableUK, Offshore Wind Energy in the UK, n.d.
[10] A.J. Kolios, M. Collu, A. Chahardehi, F.P. Brennan, M.H. Patel, A Multi-Criteria Decision Making Method to Compare Support Structures for Offshore Win d Turbines, in: EWEC 2010 Conf., Warsow, Poland, n.d.
[11] A.C. Levitt, W. Kempton, A.P. Smith, W. Musial, J. Firestone, Pricing offshore wind power, Energy Policy. 39 (2011) 6408–6421, http://dx.doi.org/10.1016/j.enpol.2011.07.044.
[12] C. Moné, A. Smith, B. Maples, M. Hand, 2013 Cost of Wind Energy Review, Nrel/Tp-5000-63267. (2013) NREL/TP-5000-63267.
[13] M.J. Kaiser, B.F. Snyder, Offshore Wind Energy Cost Modelling. Installation and Decommissioning, Springer L, London, UK, 2012, doi:10.1007/978-1-4471-2488-7.
[14] S. Koch, G. Andersson, Assessment of revenue potentials of ancillary service provision by flexible unit portfolios, 2012.
[15] P. Härtel, M. Doering, M. Jentsch, C. Pape, K. Burges, R. Kuwahata, Cost assessment of storage options in a region with a high share of network congestions, J. Energy Storage. 8 (2016) 358–367.

[16] M.H. Giahi, A. Jafarian, Dehkordi, Investigating the influence of dimensional scaling on aerodynamic characteristics of wind turbine using CFD simulation, Renew. Energy. 97 (2016) 162–168, http://dx.doi.org/10.1016/j.renene.2016.05.059.
[17] API Recommended Practice 2GEO/ISO 19901–4, Geotechnical and Foundation Design Considerations, n.d.
[18] DET NORSKE VERITAS AS, DNV RP-C202 Buckling Strength of Shells, 2013.
[19] DNV, Risk based inspection of o shore topsides static mechanical equipment. RP-G101, 2009.
[20] W. Shi, H. Park, J. Han, S. Na, C. Kim, A study on the effect of different modeling parameters on the dynamic response of a jacket-type offshore wind turbine in the Korean Southwest Sea, Renew. Energy. 58 (2013) 50–59, http://dx.doi.org/10.1016/j.renene.2013.03.010.
[21] Densit, Ultra High performance grout - Ducorit Data Sheet, (n.d.). http://www.densit.com/Files/Billeder/Densit_v2/Pdf files/renewable/pro_ducorit_itw-uk.pdf (accessed February 10, 2016).
[22] E. Winkler, Die Lehre Von Elastizitat Und Festigkeit, Dominicius, Prag, 1867.
[23] C. Koukoura, A. Natarajan, A. Vesth, Identification of support structure damping of a full scale offshore wind turbine in normal operation, Renew. Energy. 81 (2015) 882–895, http://dx.doi.org/10.1016/j.renene.2015.03.079.
[24] A. Kezdi, Handbook of Soil Mechanics, Elsevier, Amsterdam, 1974.
[25] W.-F. Chen, L. Duan, Bridge Engineering Handbook, CRC Press, USA, 1999.
[26] N. Gerolymos, G. Gazetas, Winkler model for lateral response of rigid caisson foundations in linear soil, Soil Dyn. Earthq. Eng. 26 (2006) 347–361.
[27] M. Heidari, H. El Naggar, M. Jahanandish, A. Ghahramani, Generalized cyclic p–y curve modeling for analysis of laterally loaded piles, Soil Dyn. Earthq. Eng. 63 (2014) 138–149, http://dx.doi.org/10.1016/j.soildyn.2014.04.001.
[28] K. Abdel-Rahman, M. Achmus, Finite element modelling of horizontally loaded monopile foundations for offshore wind energy converters in Germany, Hannover, 2005.
[29] H. Matlock, Correlations for Design of Laterally Loaded Piles in soft Clay, in: 2nd Offshore Technol. Conf., Houston, Texas, USA, 1970.
[30] W. Carswell, S.R. Arwade, D.J. DeGroot, A.T. Myers, Natural frequency degradation and permanent accumulated rotation for offshore wind turbine monopiles in clay, Renew. Energy. 97 (2016) 319–330, http://dx.doi.org/10.1016/j.renene.2016.05.080.
[31] S.S. Rajashree, R. Sundaravadivelu, Degradation model for one-way cyclic lateral load on piles in soft clay, Comput. Geotech. 19 (1996) 289–300.
[32] International Electrotechnical Commission, IEC 61400–1 International Satandard. Wind turbines - Part 1: Design Requirements, Geneva, Switzerland, 2005. doi:10.5594/J09750.
[33] International Electrotechnical Commission, International Standard IEC 61400–3 Wind turbines - Part 3: Design requirements for offshore wind turbines, 2009.
[34] J. Palutikof, B. Brabson, D. Lister, S. Adcock, A review of methods to calculate extreme wind speeds, Meteorol. Appl. 6 (1999) 119–132, http://dx.doi.org/10.1017/S1350482799001103.
[35] T. Sarpkaya, Wave Forces on Offshore Structures, Cambridge, Cambridge, 2010, https://www.cambridge.org/core/books/wave-forces-on-offshore-structures/0B3E4B7394C60645E7B05CEA6906322A.
[36] DNV (Det Norske Veritas), DNV−OS−J101 Design of Offshore Wind Turbine Structures, n.d.
[37] W. Carswell, J. Johansson, F. Løvholt, S.R. Arwade, C. Madshus, D.J. Degroot, A.T. Myers, Foundation damping and the dynamics of offshore wind turbine monopiles, Renew. Energy. 80 (2015) 724–736, http://dx.doi.org/10.1016/j.renene.2015.02.058.
[38] Siemens, SWT-3.6-107 Wind Turbine, 2010. http://www.energy.siemens.com/us/pool/hq/power-generation/renewables/wind-power/wind turbines/E50001-W310-A103-V6-4A00_WS_SWT_3_6_107_US.pdf.
[39] P. Passon, Damage equivalent wind e wave correlations on basis of damage contour lines for the fatigue design of offshore wind turbines, Renew. Energy. 81 (2015) 723–736, http://dx.doi.org/10.1016/j.renene.2015.03.070.
[40] M.W. LaNier, LWST Phase I Project Conceptual Design Study: Evaluation of Design and Construction Approaches for Economical Hybrid Steel/Concrete Wind Turbine Towers, Denver, Colorado, USA, 2005.
[41] F. Brennan, I. Tavares, Fatigue design of offshore steel monopile wind substructures, Proc. Inst. Civ. Eng. - Energy. 167 (2014) 1–7.
[42] Det Norske Veritas, Fatigue Design of Offshore Steel Structures, 2005. ftp://128.84.241.91/tmp/MSE-4020/Fatigue-Design-Offshore.pdf.
[43] O. Adedipe, F. Brennan, A.J. Kolios, Review of Corrosion Fatigue in Offshore Structures: Present Status and Challenges in the Offshore Wind Sector, Renew. Sustain. Energy Rev. 61 (2016) 141–154.
[44] S. Novoselac, T. Ergić, P. Baličević, Linear and Nonlinear Buckling and Post Buckling Analysis of a Bar With the Influence of Imperfections, Teh. Vjesn. 19 (2012) 695–701.
[45] M. Życzkowsky, Post-buckling analysis of non-prismatic columns under general behaviour of loading, Int. J. Non. Linear. Mech. 40 (2005) 445–463.
[46] European Standard, EN 1993-1-1 Eurocode 3: Design of steel structures - Part 1–1: General rules and rules for buildings, 2005.
[47] European Standard, EN 1993-1-6 Eurocode 3 - Design of steel structures - Part 1–6: Strength and stability of shell structures, 2007.
[48] M. Martinez Luengo, A. Kolios, L. Wang, Structural Health Monitoring of Offshore Wind Turbines: A review through the Statistical Pattern Recognition Paradigm, Renew. Sustain. Energy Rev. 64 (2016) 91–105.
[49] W. Weijtjens, T. Verbelen, G. De Sitter, C. Devriendt, Foundation structural health monitoring of an offshore wind turbine — a full-scale case study, Struct. Heal. Monit. 15 (2016) 389–402, http://dx.doi.org/10.1177/1475921715586624.
[50] C. Devriendt, F. Magalhães, W. Weijtjens, G. De Sitter, Á. Cunha, P. Guillaume, Automatic identification of the modal parameters of an offshore wind turbine using state-of-the-art operational modal analysis, in: 5th Int. Oper. Modal Anal. Conf., Guimarães, Portugal, n.d.: pp. 1–12.
[51] C. Devriendt, F. Magalhaes, W. Weijtjens, G. De Sitter, A. Cunha, P. Guillaume, Structural Health Monitoring of offshore wind turbines using automated operational modal analysis, Struct. Heal. Monit. 13 (2014) 644–659, http://dx.doi.org/10.1177/1475921714556568.
[52] A. Stahlmann, Numerical and Experimental Modeling of Scour at Tripod Foundations for Offshore Wind Turbines 1 (2014) 1019–1026.
[53] D. Rudolph, K. Bos, A. Luijendijk, K. Rietema, J. Out, Scour around offshore structures, analysis of field measurements, in: Proc 2nd Int Conf Scour Eros., Meritus Mandarin, Singapore, 2004: p. 400–407.
[54] M. Rambabu, S.N. Rao, V. Sundar, Current-induced scour around a vertical pile in cohesive soil, Ocean Eng. 30 (2003) 893–920, http://dx.doi.org/10.1016/S0029-8018(02)00063-X.
[55] L. Chen, W.H. Lam, Methods for predicting seabed scour around marine current turbine, Renew. Sustain. Energy Rev. 29 (2014) 683–692, http://dx.doi.org/10.1016/j.rser.2013.08.105.
[56] B. Mutlu, Sumer, Mathematical modelling of scour: A review, J. Hydraul. Res. 45 (2007) 723–735, http://dx.doi.org/10.1080/00221686.2007.9521811.
[57] S. Yoshida, Wind Turbine Tower Optimization Method Using a Genetic Algorithm, Wind Eng. 30 (2006) 453–469, http://dx.doi.org/10.1260/030952406779994150.
[58] D. Daniel Stratton, Martino, F.M. Pasquali, K. Lewis, J.F. Hall, A Design Framework for Optimizing the Mechanical Performance, Cost, and Environmental Impact of a Wind Turbine Tower, J. Sol. Energy Eng. 138 (2016), http://dx.doi.org/10.1115/1.4033500.
[59] Tuan-Cuong Nguyen, T.-C. Huynh, J.-T. Kim, Numerical evaluation for vibration-based damage detection in wind turbine tower structure, Wind Struct 21 (2015) 657–675.
[60] P.E. Uys, J. Farkas, K. Jármai, F. van Tonder, Optimisation of a steel tower for a wind turbine structure, Eng. Struct. 29 (2007) 1337–1342, http://dx.doi.org/10.1016/j.engstruct.2006.08.011.
[61] H.M. Negm, K.Y. Maalawi, Structural design optimization of wind turbine towers, Comput. Struct. 74 (2000) 649–666, http://dx.doi.org/10.1016/S0045-7949(99)00079-6.
[62] M.B. Zaaijer, Foundation modelling to assess dynamic behaviour of offshore wind turbines, Appl. Ocean Res. 28 (2006) 45–57, http://dx.doi.org/10.1016/j.apor.2006.03.004.
[63] W. Sahasakkul, H. Nguyen, D. Ph, A. Sari, D. Ph, An improved methodology on design and analysis of offshore wind turbines supported by monopiles, in: Offshore Technol. Conf., Houston, Texas, USA, n.d. doi:10.4043/27181-MS.

[64] W. Weijtjens, T. Verbelen, G. De Sitter, C. Devriendt, Foundation structural health monitoring of an offshore wind turbine: a full-scale case study, Struct. Heal. Monit. (2015), http://dx.doi.org/10.1177/1475921715586624.
[65] V. Negro, J.S. López-Gutiérrez, M.D. Esteban, C. Matutano, Uncertainties in the design of support structures and foundations for offshore wind turbines, Renew. Energy. 63 (2014) 125–132, http://dx.doi.org/10.1016/j.renene.2013.08.041.
[66] P. de Schoesitter, S. Audenaert, L. Baelus, A. Bolle, A. Brown, L. Das Neves, T. Ferradosa, P. Haerens, F.T. Pinto, P. Troch, R. Whitehouse, Feasibility of a dynamically stable rock armour layer scour, in: Proc. ASME 2014 33rd Int. Conf. Ocean. Offshore Arct. Eng. OMAE2014, June 8–13, 2014, San Francisco, California, USA, 2014: pp. 1–9.
[67] M. Martinez Luengo, A. Kolios, Failure Mode Identification and End of Life Scenarios of Offshore Wind Turbines: A Review, Energies 8 (2015) 8339–8354, http://dx.doi.org/10.3390/en8088339.

Parametric FEA modelling of offshore wind turbine support structures: towards scaling-up and CAPEX reduction

Martinez-Luengo, Maria

2017-05-26

Maria Martinez-Luengo, Athanasios Kolios, Lin Wang, Parametric FEA modelling of offshore wind turbine support structures: Towards scaling-up and CAPEX reduction, International Journal of Marine Energy, Volume 19, September 2017, Pages 16-31

http://dspace.lib.cranfield.ac.uk/handle/1826/11996